Hyperfine Interactions 62(1990)311 – 324

ANALYSIS OF PERTURBED ANGULAR CORRELATION SPECTRA OF METAL IONS BOUND TO PROTEINS WITH ROTATIONAL CORRELATION TIMES IN THE INTERMEDIATE REGION

E. DANIELSEN and R. BAUER

Department of Mathematics and Physics, Royal Veterinary and Agricultural University, Thorvaldsensvej 40, DK-1871 Frederiksberg C, Denmark

Received 29 October 1990; accepted 5 March 1991

The formulation by Dattagupta of the strong-collision model, describing the effect on the perturbation function, $G_2(t)$ by the isotropic tumbling of an electric field gradient, is generalized to electric field gradients with no axial symmetry. The effect on the perturbation function by strong collisions is compared to the effect of rotational diffusion in the adiabatic limit. The comparison is carried out for decays with an intermediate state of spin 5/2 and for non-axially symmetric electric field gradients. It shows that the strong-collision model can be used for interpretation of PAC spectra of molecules with correlation times between the adiabatic and the fast relaxation limits. The strong-collision model is then used to determine the rotational diffusion of the cadmium substituted copper,zinc superoxide dismutase at 3 °C and 25 °C from ^{111m}Cd TDPAC spectra. For these analyses, the model is incorporated into a conventional least-squares fitting routine.

1. Introduction

The technique of Perturbed Angular Correlations of γ-rays (PAC) is based on the detection of the angular correlation of two γ-rays emitted from the same nucleus. Usually, this angular correlation is measured as a function of the time between the two emissions (Time Differential Perturbed Angular Correlations (TDPAC)). A detailed treatment of the theory of PAC has been given by Frauenfelder and Steffen [1]. Reviews with special emphasis on chemical applications are given by Lerf and Butz [2] and Rinneberg [3].

One of the advantages of applying PAC to problems of a biological nature or origin is that experiments can be carried out on molecules in aqueous solution. Studies of the function of molecules under conditions that are close to in vivo conditions therefore become possible. This, however, leaves the problem of how to account for the effect on the perturbation function by the Brownian rotation of the molecules. For most biological work, the perturbation function must be known also for molecules with a non-axial symmetric electric field gradient.

The most popular isotopes for biologically related work are ^{111m}Cd, ^{111}In and ^{181}Hf. These all have an intermediate level of spin 5/2 and, therefore, we restrict

© J.C. Baltzer AG, Scientific Publishing Company

ourselves to this case in the following. In aqueous solution, the molecules are isotropically oriented. This means that instead of the perturbation function $G_{k_1k_2}^{N_1N_2}(t)$, only the angular averages $G_k(t)$ are measured (for the mentioned isotopes, only $k = 2$ has to be considered). For molecules reorienting slowly, the Debye model [4] results in an analytical expression for $G_2(t)$. This is also the case for molecules with a fast rotational diffusion, and in both limits this model can, therefore, be implemented directly in conventional programmes for least χ^2 data analysis. For molecules with rotational diffusion times in the intermediate region, it has been suggested by Rinneberg [3] that the strong-collision model is used to interpolate between slow and fast rotational diffusion. The model, however, leads to an integral equation that can only be solved by iteration. In general, this will make data analysis too time-consuming for most computers and scientists. It has been the aim of the present work to investigate to what extent the strong-collision model and the Debye model give the same results. Furthermore, we wanted to find a way of implementing the strong-collision model in a conventional program for least-squares fitting. The application is illustrated by the study of the rotational correlation of copper,zinc-superoxide dismutase ($Cu(II)_2Zn_2SOD$) from yeast. This enzyme was chosen because the static interaction of Cd^{2+} in the cadmium substituted enzyme ($Cu(II)_2Cd_2SOD$) is well characterised [5,6], and because the calculated correlation time is well into the intermediate region.

In the case where the nuclei experiences no magnetic field, the interaction of the nucleus with the electric field gradient caused by the surroundings can be characterised by the strength of the nuclear quadrupole interaction ω_0 defined as:

$$\omega_0 = \frac{12\pi |V_{zz} eQ|}{40h} \tag{1}$$

and the asymmetry parameter η defined as $\eta = (V_{xx} - V_{yy})/V_{zz}$. V_{aa} is the ath diagonal component of the electric field gradient in the principal coordinate system, where V_{ab} is diagonal and $|V_{zz}| \geq |V_{yy}| \geq |V_{xx}|$, and Q denotes the electric quadrupole moment of the nucleus. Also, a Gaussian distribution of ω_0 in the sample, described by the relative width $\delta = \Delta\omega_0/\omega_0$, is taken into account. These parameters describe the interaction of the nucelus with the surroundings if the molecule does not undergo reorientation.

2. Models describing molecular reorientation in liquids

2.1. THE JUMP DIFFUSION MODEL

The "Debye model" and the "strong-collision model" can be considered as two extreme cases of the jump diffusion model. In the jump diffusion model, the molecule reorients by a series of discontinuous jumps. Following the formulation by Berne and Pecora [7], the assumptions are:

(a) The jump takes place instantaneously.

(b) Successive jumps are uncorrelated in time with an average time τ_v between jumps. (The probability that a jump occurs between t and $t + dt$ is dt/τ_v.)

(c) The dihedral angle between the two planes defined by the orientation vector $\boldsymbol{u}$ in two successive jumps is randomized.

2.2. THE STRONG-COLLISION MODEL

In this model, the distribution function of jump angles is uniform, each collision leading to a complete loss of memory of the original orientation. The advantage of this model is that it leads to a simple form for calculating the perturbation function, irrespective of the correlation time τ_v (vide infra).

2.3. THE DEBYE MODEL

The case where the distribution function of jump angles is peaked at small angles corresponds to the Debye model. The Debye model [4] is based on the assumption that collisions are so frequent in a liquid that a molecule can only rotate through a very small angle before suffering a reorienting collision. In contrast to the strong-collision model, the Debye model allows for asymmetric diffusion. The diffusion is described by the rotational diffusion tensor θ_{ij}. The body-fixed axes can be chosen so that θ_{ij} is diagonal:

$$\theta = \begin{pmatrix} \theta_{xx} & 0 & 0 \\ 0 & \theta_{yy} & 0 \\ 0 & 0 & \theta_{zz} \end{pmatrix}. \tag{2}$$

For a spherical rotor ($\theta_{xx} = \theta_{yy} = \theta_{zz} \equiv \theta$), the correlation time τ_l is $\tau_l = (\theta(l + 1)l)^{-1}$ [8], where l is the moment of the tensor describing the measured quantity. In general, l will depend on the technique used to determine the rotational correlation. In PAC experiments applied to isotropically oriented molecules, only even values of l are measured through the perturbation functions $G_l(t)$. For PAC utilising the isotopes ^{111m}Cd, ^{111}In or ^{181}Hf, the perturbation function $G_2(t)$ is measured and the corresponding correlation time of a spherical rotor is $\tau_2 = 1/6\theta$. This is also the case for fluorescence depolarization, dynamic light scattering and NMR, whereas in dielectric spectroscopy, $l = 1$ and $\tau_1 = 1/2\theta$. A review of some of the techniques used for studying the dynamics of thermal fluctuations in fluids is given by Berne and Pecora [7]. The dependence of the correlation time on the technique is an important contrast of the Debye model to the strong-collision model in which the correlation time by definition is τ for all moments.

3. Effect on perturbed angular correlation of γ-rays by molecular reorientation

3.1. THE EFFECT OF THE DEBYE-MODEL ON THE PERTURBATION FUNCTION

In general, the effect of the diffusion on the perturbation function will depend on the orientation of the diffusion tensor θ_{ij} with respect to the electric field gradient tensor V_{ab}. Here, only the influence of a spherical rotor on the PAC spectrum will be treated.

This problem was solved in the extreme narrowing limit ($\omega_0\tau \ll 1$) by Abragam and Pound [9] for $\eta = 0$. In this limit, the perturbation function is:

$$G_2(t) = e^{-2.8\,\omega_0^2\tau t}, \qquad \eta = 0;\ \omega_0\tau \ll 1. \tag{3}$$

The effect on the perturbation function of a motion in the adiabatic limit ($\omega_0\tau \gg 1$) has been treated by Marshall et al. [10]. This limit gives:

$$G_2(t) = e^{-t/\tau} G_2^0(t), \qquad \eta = 0;\ \omega_0\tau \gg 1, \tag{4}$$

where $G_2^0(t)$ is the perturbation function for the static interaction. This formula is valid for $\eta \neq 0$ as well (appendix A). Marshall et al. [10] also treat the rotational diffusion of the asymmetric top molecule in the adiabatic limit and, for the extreme narrowing limit, draw attention to the proportionality of $1/T_1$ (T_1 is the relaxation time measured by NMR) and the decay constant of the angular correlation in PAC. This means that the derivations by Huntress [11] for NMR are immediately applicable to PAC. Of special interest for the present work is the result of a spherical rotor and an asymmetric electric field gradient:

$$G_2(t) = e^{-2.8\,\omega_0^2\tau(1+\eta^2/3)t}, \qquad \omega_0\tau \ll 1. \tag{5}$$

In the intermediate region ($\omega_0\tau \approx 1$), no analytical expression exists for the perturbation function $G_2(t)$. A general formulation of the problem is given by Winkler and Gerdau [12, 13], who solved the problem by solving the eigenvalue problem of a 108×108 matrix (intermediate spin 5/2). For an axial symmetric electric field gradient, the dimension of the matrix reduces to 23×23. This formulation has been used by Winkler [13] to calculate the perturbation function $G_2(t)$ for $\eta = 0$ for a number of different correlation times.

3.2. THE EFFECT OF THE STRONG-COLLISION MODEL ON THE PERTURBATION FUNCTION

This model was first applied to perturbed angular correlations by Scherer [14] and Blume [15]. It leads to a very simple expression for the Laplace transform of the perturbation function

$$\tilde{G}_k(p) = \int_0^\infty \mathrm{e}^{-pt} G_k(t)\,\mathrm{d}t,$$

$$\tilde{G}_k(p) = \frac{\tilde{G}_k^0(p + 1/\tau)}{1 - (1/\tau)\tilde{G}_k^0(p + 1/\tau)}, \tag{6}$$

where $\tilde{G}_k^0(p)$ is the Laplace transform of the static perturbation function $G_k^0(t)$.

We have used the numerical technique for computation of $G_2(t)$ proposed by Dattagupta [16]. Dattagupta has used the above equation to derive the integral equation:

$$\frac{\mathrm{d}G_2(t)}{\mathrm{d}t} = -\int_0^t K_2^0(t`)\mathrm{e}^{-\lambda t`} G_2(t - t`)\,\mathrm{d}t`, \tag{7}$$

where λ denotes the orientational decay constant defined as $1/\tau$. $K_2^0(t`)$ is independent of λ and, therefore, can be found by solving the above equation for the known static perturbation factor. An inspection of the proof by Dattagupta and Blume [17] shows that this way of computing the perturbation function can be generalized to include cases where $\eta \neq 0$ (see appendix B).

The result of solving the above equation is shown for $\eta = 0$ and $\eta = 0.4$ in fig. 1 for a number of different λ. The correlation times are chosen such that the result for $\eta = 0$ can be compared to the result obtained by Winkler using the matrix method [13]. The $(1 + \eta^2/3)$ dependence in η for fast rotations is seen in fig. 1, where the perturbation functions for $\eta = 0.4$ and $\eta = 0$ almost coincide at $\lambda = 25\,\omega_0/2\pi$, whereas $\eta = 0.8$ still can be distinguished from the two others.

3.3. COMPARISON OF THE EFFECT OF THE DEBYE MODEL AND THE STRONG-COLLISION MODEL

In order to use the strong-collision model to interpret spectra measured on molecules with a rotational correlation time between the adiabatic and the extreme narrowing limit, it is necessary to compare the results of the two models in the two limits. This has been done by Lynden-Bell [18], who finds that the two models predict the same result in the fast rotational limit if $6\theta = 1/\tau$. This is in accordance with an $l = 2$ interaction, and is also valid for electric field gradients with no axial symmetry. In the slow rotational limit, Lynden-Bell finds that for $\eta = 0$ the perturbation factor resulting from the strong-collision model can be approximated by the Debye model if $7\theta \approx 1/\tau$.

We have computed the two models for $\omega_0\tau = 12.5$ for $\eta \in [0; 1]$. The comparison shows that in the range of $\omega_0 t$ between 0 and 16, the perturbation function based

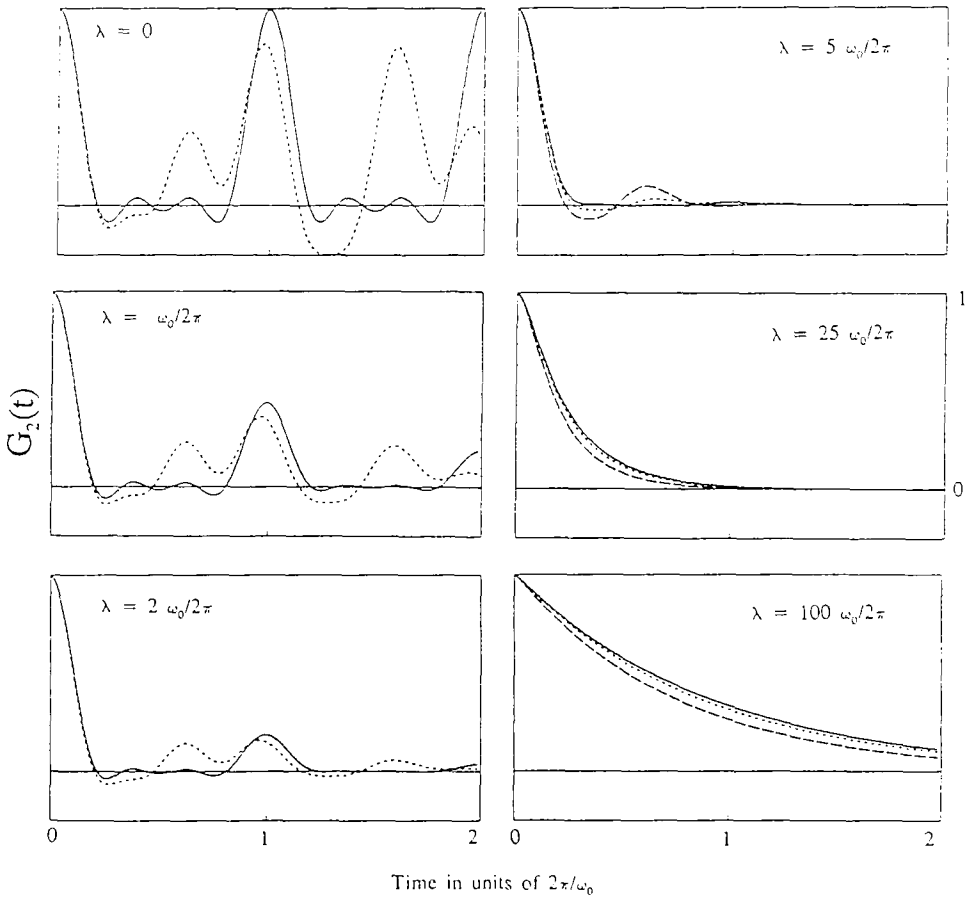

Fig. 1. Perturbation functions $G_2(t)$ for a nucleus of spin = 5/2 under the influence of an electric quadrupole interaction randomly reorienting by strong collisions. The perturbation functions are calculated for $\eta = 0$ (——) and 0.4 (- - - -). In addition, $\eta = 0.8$ is shown for $\lambda = 5\omega_0/2\pi$, $25\omega_0/2\pi$ and $100\omega_0/2\pi$ (– – –).

on the strong-collision model can be approximated by the Debye model, giving $1/\tau$ between 7.1θ and 8.2θ depending on η.

The largest deviation between the two models was found for an asymmetry of about 0.8. This is shown in fig. 2 for $\omega_0 = 100$ Mrad/s and $\lambda = 0.008$ ns^{-1} in the strong-collision model. The parameters of the Debye model were the same except for the correlation time τ, which was varied to give the smallest possible integrated deviation between the two functions from 0 to 160 ns. This gave a rotational diffusion of $1/\tau = 0.006$ ns^{-1} for the optimized Debye model.

We do not expect to be able to distinguish the two models experimentally. However, when used for data analysis, a soft transition between the two model was used. As an additional test of the computational method, it was checked that the

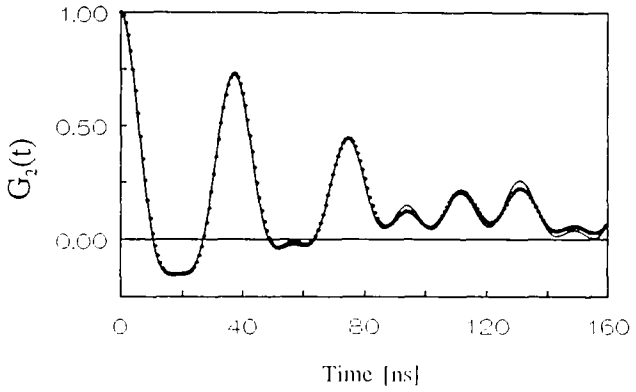

Fig. 2. The strong-collision model (•) (λ = 0.008 ns^{-1}) is compared to the Debye model (–) (λ = 0.006 ns^{-1}) for ω_0 = 100 Mrad/s, and η = 0.8.

strong-collision model gave the predicted result (eq. (5)) in the fast rotation limit for all values of η.

4. Experimental

The effect on the rotational diffusion on the TDPAC spectrum is illustrated by $Cu(II)_2Cd_2SOD$.

The experiments were carried out on the enzyme used by Bauer et al. [19]. The apo-enzyme has been kept dehydrated in a refrigerator.

The radioactive ^{111m}Cd was produced as described by Bauer et al. [5]. For each experiment, 3.2 mg of apoSOD was resolved in 1 ml 0.1 M MES (2(N-morpholino) ethanesulfonic acid) buffer pH 6. To ensure that all copper sites were occupied, this was mixed with 2.5 moles of Cu^{2+} ions per mole of metal-free SOD. After at least 5 minutes, the solution was mixed with 0.25–0.5 moles of Cd^{2+} per mole of enzyme (^{111m}Cd and carrier cadmium). The TDPAC spectrum of the enzyme was then measured in 52% sucrose (w/w) at 3 °C ± 1 °C (two experiments) and without sucrose at 3 °C ± 1 °C (two experiments) and at 25 °C ± 1 °C, respectively. For the experiments without sucrose, the enzyme was filtered (0.2 μm filter) before it was mixed with the cadmium. This was done to remove possible aggregates.

The experiments were carried out on a conventional slow–fast set-up using four BaF_2 detectors with a diameter of 5.08 cm and length of 5.08 cm, arranged in a plane at fixed angles 0° (1), 90° (2), 180° (3) and 270° (4). Eight different spectra were collected: four which are forward in time and four backwards. After time reversal and background subtraction, the following expression is derived:

$$A_{2\,\mathrm{eff}}G_2(t) = \frac{\sqrt{W_{42}\cdot W_{31}} - \sqrt{W_{41}\cdot W_{32}}}{\sqrt{W_{42}\cdot W_{31}} + 2\sqrt{W_{41}\cdot W_{32}}} + \frac{\sqrt{W_{24}\cdot W_{13}} - \sqrt{W_{23}\cdot W_{14}}}{\sqrt{W_{24}\cdot W_{13}} + 2\sqrt{W_{23}\cdot W_{14}}}, \quad (8)$$

where W_{ij} denotes the coincidence spectrum after background subtraction and time reversal (only the first four spectra) of 150 keV γ-rays in detector i and 247 keV γ-rays in detector j.

The effective amplitude $A_{2\,\mathrm{eff}}$ was about 10%. Before each experiment, the spectrometer was time-calibrated and the time resolution was determined using a ^{75}Se source. The time resolution was about 1.9 ns. The temperature was controlled by a Peltier element.

5. Data analysis

For data analysis, the rotational diffusion was divided into three regions: $\ln(\lambda/\omega_0) \leq -2.5$; $-2.5 \leq \ln(\lambda/\omega_0) \leq 2.25$ and $2.25 \leq \ln(\lambda/\omega_0)$.

The modelling function for $\ln(\lambda/\omega_0) \leq -2.5$ was:

$$G_2(t) = \mathrm{e}^{-\lambda t} \sum_{i=0}^{3} S_{2i}(\eta)\mathrm{e}^{-\omega_i^{`2}\left(\frac{\tau_0^2}{16\ln 2} + \frac{t^2\delta^2}{2}\right)}\cos(\omega_i^{`} t), \tag{9}$$

where λ is the rotational diffusion parameter, $S_{2i}(\eta)$ denotes the η-dependent amplitudes of the four frequencies (the first frequency is 0), $\omega_i^{`}$ is the ith (η dependent) frequency, τ_0 is the FWHM (full width to half maximum) of the time resolution of the spectrometer and δ is the relative line width of the (Gaussian) distribution of frequencies (ω_0). (For the definitions of ω_0 and η, please refer to the introduction.) For $\ln(\lambda/\omega_0) \geq 2.25$, the following modelling function was used:

$$G_2(t) = \frac{\exp\left(-\dfrac{\omega_0^2 kt}{\lambda + 2\delta^2 kt}\right)}{\sqrt{1 + \dfrac{2\delta^2 kt}{\lambda}}}, \tag{10}$$

where $k = 2.8\ (1 + \eta^2/3)$. This function is the result of folding equation (5) with a Gaussian distribution (width δ) of nuclear quadrupole interaction strengths centered at ω_0.

In the range where $-2.5 \leq \ln(\lambda/\omega_0) \leq 2.25$, the strong-collision model was used. To solve the integral equation for each iteration in a least-squares fitting routine would be too time consuming. Instead, the integral equation was solved for 200 values of $\omega_0 t$ from $\omega_0 t = 0$ to $\omega_0 t = 40$; for 21 values of η from 0 to 1 in steps of 0.05; and for 20 values of $\ln(\lambda/\omega_0)$ ranging from -2.5 to 2.25 in steps of 0.25. Both $G_2(t)$ and $\mathrm{d}G_2(t)/\mathrm{d}t$ were calculated for this $200 \times 20 \times 21$ parameter set. This was then installed in the memory of a μVAX(II) computer, used for data analysis.

The perturbation function was then calculated by interpolation in $\omega_0 t$, η and λ for a given set of parameters. The interpolation was a third-order polynomial

interpolation in $\omega_0 t$ using $G_2(\omega_0 t)$ and $\mathrm{d}G_2(\omega_0 t)/\mathrm{d}t$ for the two nearest values of $\omega_0 t$. This was followed by a second-order interpolation in η, and finally a second-order polynomial interpolation in λ carried out on $\ln | G_2(\omega_0 t) |$ using the known exponential dependence in λ for small λ (if $G_2(\omega_0 t)$ changed sign between the three λ's involved, the interpolation was carried out in $G_2(\omega_0 t)$).

5.1. INCORPORATION OF FREQUENCY DISTRIBUTION

To keep the dimensions of the database low, the frequency distribution was not introduced at this level. Instead, the effect of the frequency distribution was calculated by taking advantage of the fact that the frequency distribution mainly enters in the product of $\omega_0 t$. Neglecting the distribution in λ/ω_0, the effect of the frequency distribution was calculated by:

$$G_2^{\delta\tau_0}(\omega_0 t) = \frac{\int_{\max(0,\,\omega_0 t-3\Delta)}^{\omega_0 t+3\Delta} \exp(-x^2/2\Delta^2)\cdot G_2^{00}(\omega_0 t + x)\,\mathrm{d}x}{\int_{\max(0,\,\omega_0 t-3\Delta)}^{\omega_0 t+3\Delta} \exp(-x^2/2\Delta^2)\,\mathrm{d}x}, \tag{11}$$

where

$$\Delta = \sqrt{\frac{\tau_0^2\,\omega_0^2}{8\ln 2} + (\omega_0 t\delta)^2}\,.$$

$G_2^{00}(t)$ is the corresponding perturbation function without frequency distribution and with infinitely good time resolution. The advantage of this approach is that $G_2^{00}(t)$ has already been calculated.

To ensure a smooth χ^2 surface, the borderline between the use of the Debye model and the strong-collision model was softened by a linear combination of the two models.

6. Results

The spectra are shown in fig. 3 and fig. 4. The result of the least-squares data analysis of the sucrose spectrum was $\omega_0 = 150.2 \pm 0.4$ Mrad/s, $\eta = 0.25 \pm 0.01$, $\lambda = 0.0070 \pm 0.0007$ ns^{-1} and no frequency distribution. These values of ω_0 and η were used for the data analysis of the two spectra shown in fig. 4. The least-squares data analysis gave $\lambda = 0.093 \pm 0.016$ ns^{-1} (25 °C) and $\lambda = 0.064 \pm 0.007$ ns^{-1} (3 °C), respectively.

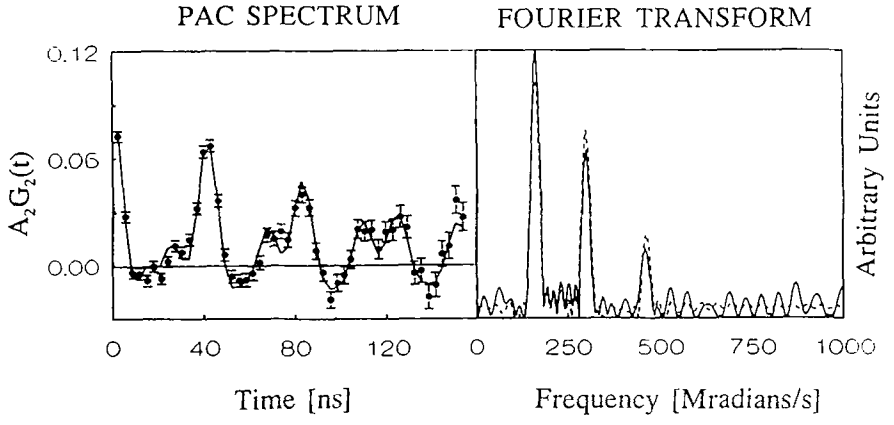

Fig. 3. TDPAC spectrum of $Cu(II)_2Cd_2SOD$ measured at 3 °C in 52% sucrose. The full line shows the result of a least-squares fit. The Fourier transform is shown for the data points (full line) as well as for the fitted curve (broken line). The data points represent the average of four experimental points. The bars indicate standard deviations.

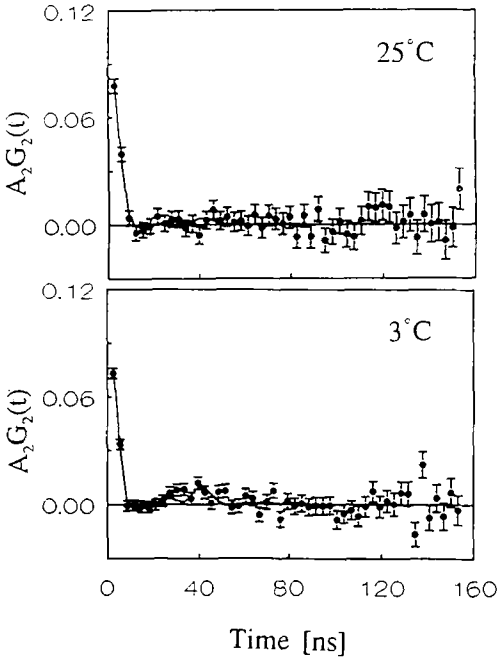

Fig. 4. TDPAC spectra of $Cu(II)_2Cd_2SOD$ measured at 25 °C and 3 °C.

The nuclear quadrupole interation of the sucrose experiment is, within the experimental uncertainty, in agreement with the yeast $Cu(II)_2Cd_2SOD$ nuclear quadrupole interaction stated in [5,6]. This shows that the procedure used places the cadmium ions in the zinc site with the neighbouring copper site occupied by a Cu(II)-ion. The correlation times of the two experiments at 25 °C and 3 °C are 10.7 ± 1.8 ns and 15.6 ± 1.8 ns.

7. Conclusion

If one assumes that the enzyme can be approximated by a spherical molecule of the same mass and a hydrated volume of 1.07×10^{-3} m^3/kg (average of several proteins [20]), the rotational correlation time can be calculated as: $\tau = (6\theta)^{-1} = V\xi/(kT)$ [4], where V is the hydrated volume, ξ is the viscosity of the solvent and T is the absolute temperature.

Using the molecular weight 32000 and the viscosity of water [21], the calculated values are: 12.3 ns (25 °C) and 24.2 ns (3 °C). The correlation time measured at 25 °C without sucrose is thus in agreement with the calculated value, whereas the value measured at 3 °C is about 30% lower than the calculated value. The analyses of these experiments made the use of the strong-collision model necessary, since $\omega_0\tau$ is 1.6 and 2.34, respectively.

The above described method provides a means of analysing PAC spectra from molecules with spherical rotational motion. The interpolation by the strong-collision model between the slow and fast rotational diffusion regions may lead to an error of about 20% in the interpretation of λ. For quadrupole interactions without frequency distribution, the use of the database does not give cause to any slowing down of the fitting programme. For frequency distributions of 7%, the programme is slowed down by about a factor of 3 compared to the analytical expressions used in the adiabatic region. If the frequency distribution is known for the probe, it might be incorporated in the database to save time.

Instead of using the strong-collision model in the intermediate region, it should be possible to use the Debye model by calculating $G_2(t)$ for a large but limited number of λ and η. This is possible using the method of Winkler [13] forming and solving the eigenvalue problem of a 108×108 matrix.

Appendix A

ROTATIONAL DIFFUSION OF A NON-AXIALLY SYMMETRIC QUADRUPOLE INTERACTION IN THE ADIABATIC LIMIT

Following the proof by Marshall and Meares [22] but including electric field gradients of non-axial symmetry, one has to express the orientation of the electric field gradient by all three rotation angles, α, β and γ. Furthermore, as the m-states in the principal coordinate system are not eigenfunctions of the (static) interaction

Hamiltonian, these m-states have to be expanded on the eigenstates n of the Hamiltonian. Equation (9) in [22] then generalizes to:

$$\begin{aligned}\langle G_{K_1K_2}^{N_1N_2}(t)\rangle = \sqrt{(2K_1+1)(2K_2+1)} \sum_{\substack{n,n',m_1,m_1',m_1'',\\ m_1''',m_2,m_2',m_2'',m_2'''}} (-1)^{2I+m_1'+m_2'} \\ \times e^{-(i/h)(E_n-E_n')t}\langle n|m_2''\rangle\langle n'|m_2'''\rangle^*\langle n|m_1''\rangle^* \\ \times \langle n'|m_1'''\rangle \begin{pmatrix} I & I & K_1 \\ -m_1' & m_1 & N_1 \end{pmatrix}\begin{pmatrix} I & I & K_2 \\ -m_2' & m_2 & N_2 \end{pmatrix} \\ \times \int P(\Omega_0,\Omega_0,t) D_{m_1,m_1''}^{I}(\Omega_0) D_{m_1',m_1'''}^{*I}(\Omega_0)\,d\Omega_0 \\ \times \int P(\Omega,\Omega_0,t) D_{m_2,m_2''}^{*I}(\Omega) D_{m_2',m_2'''}^{I}(\Omega)\,d\Omega,\end{aligned} \tag{A1}$$

where $P(\Omega, \Omega_0, t)$ represents the probability that the electric field gradient is oriented in the direction Ω at time t, given it was oriented in direction Ω_0 at time zero.

Using the expression of $P(\Omega, \Omega_0, t)$ [22]:

$$P(\Omega,\Omega_0,t) = \sum_{l,m} Y_{lm}^*(\Omega) Y_{lm}(\Omega_0) e^{(-t/\tau_l)} \tag{A2}$$

and following the procedure of Marshall and Meares [22], the integration over Ω leads to the vanishing of all terms except $K_1 = l$ and $K_2 = l$. The exponential factor $\exp(-t/\tau_l)$ ($l = K_1 = K_2$) can therefore be extracted. Performing the summation, eq. (A1) then reduces to:

$$\langle G_{K_1K_2}^{N_1N_2}(t)\rangle_{AV(\alpha,\beta,\gamma,A,B,G)} = e^{(-t/\tau_l)} G_l^{\cdot}(t)\,\delta_{K_1 l}\,\delta_{K_2 l}\,\delta_{N_1 0}\,\delta_{N_2 0}, \tag{A3}$$

where $G_l^{\cdot}(t)$ is the perturbation function of the static interaction.

Appendix B

THE EFFECT OF STRONG-COLLISIONS ON THE PERTURBATION FUNCTION OF NON-AXIALLY SYMMETRIC ELECTRIC FIELD GRADIENTS

The proof of the integral equation,

$$\frac{dG_2(t)}{dt} = -\int_0^t K_2^0(t^{\cdot}) e^{-\lambda t^{\cdot}} G_2(t-t^{\cdot})\,dt^{\cdot} \tag{B1}$$

given by Dattagupta and Blume [17] and Dattagupta [16], is based only on the assumption that η is 0 in the proof of

$$\overline{U^0} = \tilde{D}\,\overline{U^0}\,\tilde{D}^{-1}, \tag{B2}$$

where the matrix elements of $\bar{U}^0$ are:

$$(I_0 m_0 I_1 m_1|\overline{U^0(p)}|I_0 m_0' I_1 m_1') = \frac{1}{4\pi}\int d\Omega_l \int_0^\infty dt\, e^{-pt}\langle I_0 m_0|e^{iV_l t}|I_0 m_0'\rangle$$

$$\times \langle I_1 m_1'|e^{-iV_l t}|I_1 m_1\rangle, \qquad \text{where } d\Omega_l = d\alpha_1 \sin\beta_1\, d\beta_1 \tag{B3}$$

and $\tilde{D}$ is the super-operator corresponding to any rotation operator $D(\alpha, \beta, \gamma)$. The symmetry of the electric field gradient is used to express the electric quadrupole interaction tensor V_l by:

$$V_l = D^{(l)}(\alpha, \beta, 0)V_z(D^{(l)})^{-1}(\alpha, \beta, 0), \tag{B4}$$

where α and β rotate the coordinate system to the orientation, where the electric field gradient is diagonal and with the principal component in the z-direction.

For non-axial symmetry, this has to be generalized to:

$$V_l = D^{(l)}(\alpha, \beta, \gamma)V_{ij}(D^{(l)})^{-1}(\alpha, \beta, \gamma), \tag{B5}$$

and the integration over all angles in eq. (B2) must be performed over all orientations described by α, β and γ. The matrix elements of $\tilde{D}\,\bar{U}^0\tilde{D}^{-1}$ then become:

$$(I_0 m_0 I_1 m_1|\tilde{D}\,\overline{U^0}(p)\tilde{D}^{-1}|I_0 m_0' I_1 m_1')$$

$$= \frac{1}{8\pi^2}\int d\Omega_l \int_0^\infty dt\, e^{-pt} \sum_{\substack{n_1 n_0 \\ n_0' n_1'}} (I_0 m_0 I_1 m_1|\tilde{D}|I_0 n_0 I_1 n_1)$$

$$\times (I_0 n_0 I_1 n_1|\overline{U^0}(p)|I_0 n_0' I_1 n_1')(I_0 n_0' I_1 n_1'|\tilde{D}^{-1}|I_0 m_0' I_1 m_1')$$

$$= \frac{1}{8\pi^2}\int d\Omega_l \int_0^\infty dt\, e^{-pt} \sum_{\substack{n_1 n_0 \\ n_0' n_1'}} \langle I_0 m_0|D|I_0 n_0\rangle\langle I_1 n_1|D^{-1}|I_1 m_1\rangle$$

$$\times \langle I_0 n_0|e^{iV_l t}|I_0 n_0'\rangle\langle I_1 n_1'|e^{-iV_l t}|I_1 n_1\rangle\langle I_0 n_0'|D^{-1}|I_0 m_0'\rangle\langle I_1 m_1'|D|I_1 n_1'\rangle$$

$$= \frac{1}{8\pi^2} \int d\Omega_l \int_0^\infty dt\, e^{-pt} \langle I_0 m_0 | D e^{iV_l t} D^{-1} | I_0 m_0' \rangle \langle I_1 m_1' | D e^{-iV_l t} D^{-1} | I_1 m_1 \rangle$$

$$= \frac{1}{8\pi^2} \int d\Omega_l \int_0^\infty dt\, e^{-pt} \langle I_0 m_0 | e^{i(DV_l D^{-1})t} | I_0 m_0' \rangle \langle I_1 m_1' | e^{-i(DV_l D^{-1})t} | I_1 m_1 \rangle, \quad \text{(B6)}$$

where $d\Omega_l = d\alpha_l \sin\beta_l\, d\beta_l\, d\gamma_l$. This of course corresponds to eq. (B3), since there is no difference between integrating over all orientations and all orientations rotated by the angles α, β and γ.

Acknowledgements

Brd. Hartmann's Foundation is acknowledged for the μVAX(II). This work was supported by the Danish Natural Science Research Council.

References

[1] H. Frauenfelder and R.M. Steffen, Angular correlations, in: *Alpha-, Beta-, and Gamma-ray Spectroscopy*, ed. K. Siegbahn, Vol. 2 (North-Holland, Amsterdam, 1965), pp. 997–1198.
[2] A. Lerf and T. Butz, Angew. Chem. Int. Ed. Engl. 26(1987)110–126.
[3] H.H. Rinneberg, Atomic Energy Rev. 172(1979)477–595.
[4] P. Debye, *Polar Molecules* (Dover, New York, 1929).
[5] R. Bauer, M.J. Bjerrum, E. Danielsen and P. Kofod, Acta Chem. Scand., Ser. A 45(1991) No. 6.
[6] R. Bauer, M.J. Bjerrum, E. Danielsen and P. Kofod, Hyp. Int. 61(1990)1201–1204.
[7] B.J. Berne and R. Pecora, *Dynamic Light Scattering* (Wiley, New York, 1976).
[8] L.D. Favro, Phys. Rev. 119(1960)53–62.
[9] A. Abragam and R.V. Pound, Phys. Rev. 92(1953)943–962.
[10] A.G. Marshall, L.G. Werbelow and C.F. Meares, J. Chem. Phys. 57(1972)364–370.
[11] W.T. Huntress, Jr., J. Chem. Phys. 48(1968)3524–3533.
[12] H. Winkler and E. Gerdau, Z. Phys. 262(1973)363–376.
[13] H. Winkler, Z. Phys. A276(1976)225–232.
[14] C. Scherer, Nucl. Phys. A157(1970)81–92.
[15] M. Blume, Nucl. Phys. A167(1971)81–86.
[16] S. Dattagupta, Hyp. Int. 11(1981)77–126.
[17] S. Dattagupta and M. Blume, Phys. Rev. B10(1974)4540–4550.
[18] R.M. Lynden-Bell, Mol. Phys. 21(1971)891–900.
[19] R. Bauer, I. Demeter, V. Haseman and J.T. Johansen, Biochem. Biophys. Res. Commun. 94, 4(1980)1296–1302.
[20] I.D. Kuntz and W. Kauzmann, Adv. Protein Chem. 28(1974)239–345.
[21] G.W.C. Kay and T.H. Laby, *Tables of Physical and Chemical Constants*, 12 ed. (Longmans, Green, London, 1959).
[22] A.G. Marshall and C.F. Meares, J. Chem. Phys. 56(1972)1226–1229.